Transmission of body sounds: an overview

E. Kaniušas

Institute of Fundamentals and Theory of Electrical Engineering Bioelectricity & Magnetism Lab,

Vienna University of Technology

Vienna, Austria, kaniusas@tuwien.ac.at

Abstract

Body sounds show a high diagnostic value when auscultated on the skin. The sound transmission from sound sources to the site of auscultation plays an important role, for it determines the signal properties of the recorded biosignal. The present paper gives an overview about the unique phenomena of spreading and attenuations of the body sounds, showing that the heterogeneous structure of the thorax and the sound frequency influence strongly the propagation pathway and characteristics of the sounds. The issues pertaining to the transmission of the body sounds provide clinically relevant insights into the correlations between the physiological phenomena under investigation and the registered biosignals and offer a solid basis for both proper understanding of the biosignal relevance and optimization of the recording techniques.

Key words: body sounds, sound propagation, sound attenuation, spreading losses, volume losses, inhomogeneity losses

1. Introduction

The body sounds have remained timeless since Laennec improved the audibility of heart and lung sounds with its wooden stethoscope, invented in 1816 [1]. The heart sounds have conveyed meaningful signals to the examiner looking for cardiac disturbances while the lung sounds have allowed for the assessment of the respiratory abnormalities. Recently, also snoring sounds gained importance, for instance, as a warning sign of sleep apnea [2, 3].

The heart sounds occur predominantly because of the valvular activity of the heart, showing spectral components in the range (0-100) Hz [2], [4]. The generation mechanisms of the lung sounds rely on more complicated biomechanical phenomena [5-9]. In particular, the tracheobronchial sounds (heard over the large airways) are primarily related to the turbulent airflow and vibrations of the upper airway walls, whereas the vesicular sounds (heard on the thorax) arise, as the air moves from larger airways into smaller ones, hitting the branches of the airways; the relevant spectral component extending up to 500 Hz. The snoring sounds are mainly generated by vibrations of the pharyngeal walls and the soft palate [10-13]. The snoring appears in the range up to approximately 1 kHz while the obstructive (apneical) snoring shows amplitudes up to 2 kHz.

Given the generation mechanisms of the different body sounds, the hypothetical sound sources of the heart sounds, tracheobronchial lung sounds, and snoring sounds can be considered, in an approximation, as remaining locally restricted to the heart region, the larger airways and the upper airways, respectively [14]. In contrast, the sources of the vesicular lung sounds are not confined to a certain region but are rather distributed within the whole periphery of the lung [5, 8, 9, 14, 15].

The present paper describes unique phenomena pertaining to the propagation of the body sounds from the respective sound source to the site of auscultation. In particular, this is relevant for a proper understanding of the relationship between the physiological activity of interest and the auscultated biosignal. Furthermore, the propagation phenomena allow significant insights into the biosignal relevance and the optimization of auscultation techniques.

2. Propagation of body sounds

The propagation of the body sounds as well as any other acoustic waves in the time and space domain is described in terms of the sound wavelength λ (spatial characteristic), the sound frequency f (time-related characteristic) and the sound velocity v (time-spatial characteristic). The value of v is determined through physical properties of the propagation medium, to give

$$v = \lambda \cdot f = \sqrt{\frac{\kappa}{\rho}} = \sqrt{\frac{1}{\rho \cdot D}} \, . \qquad (1)$$

Here κ is the module of the volume elasticity, ρ is the density of the medium, and D $(=1/\kappa)$ is the compliance or adiabatic compressibility. In the case of gases, e.g., air, κ is expressed as the product of adiabatic coefficient and gas pressure.

Obviously Eq. 1 account for the sound propagation in any type of homogeneous medium, including the biological tissue. Table 1 summarizes the values of v and λ for the most relevant types of biologic media involved in the transmission of the body sounds. One can observe that the lung parenchyma which ρ and D are given by the mixture of the tissue and the air yields a relatively low v in the order of only 50 m/s (23 m/s up to 60 m/s [8]), the value depending strongly on air content. This value is much lower as compared with v in the tissue ($\approx$1500 m/s) or in the large airways ($\approx$270 m/s) alone. As a result, the parenchyma accounts for the lowest values of λ ($\approx$5 cm at 1 kHz) which certainly decrease even more with increasing f.

2.1. Spreading of sounds

If the calculated values of λ in Table 1 are put into relation with the distance r from the body sound sources (e.g., heart valves or upper airways) to a possible auscultation site on the chest (Fig.1), then it becomes obvious that primarily the near field condition ($r<2\cdot\lambda$) prevails on the auscultation site. That is, the relevant relation $r<2\cdot\lambda$ is supported by the scaled real cross-section of the thorax, as shown in Fig.1a. It demonstrates that the practically relevant values of r are in the range (0.2-0.3)m. On the other hand, the size of the body sound sources is in the order of λ, which also supports the assumption of the near field.

One would observe that r is smaller or at least equal to λ in all types of the propagation media but not in the lung parenchyma (Table 1). The high frequency body sounds traveling through the parenchyma ($\lambda\approx2.5$ cm at $f=2$ kHz) would not meet the near field condition from above. However, as will be shown in Chapter 2.2, the high frequency body sounds tend to take airway bound route within the airway-branching structure but not the way bound to the inner mediastinum and parenchyma.

In order to discuss the propagation phenomena of the body sounds and their absorption from a more theoretical point of view, two types of prevailing sound sources can be assumed:

1. Point source of sound, as approximately given in the case of the heart sounds, tracheobronchial lung sounds, and snoring sounds;

2. Distributed sources of sound, as given for the vesicular lung sounds (Chapter 1).

Table 1. **Approximate values of the sound velocity in the air, water, muscle [16], large airways, tissue [8], tallow [17], and lung [8],[18, 19]. Corresponding wavelengths are calculated at 1 kHz. Approximate absorption coefficients are given according to the classical absorption theory [17], [20].**

	Sound velocity v (m/s)	Wavelength at 1 kHz λ (m)	Classical absorption coefficient at 1 kHz $\alpha_F + \alpha_T$ (1/m)
Air	340	0.34	10^{-5}
Large airways (diameter > 1 mm)	270	0.27	10^{-5}
Water	1400	1.4	10^{-8}
Tissue ($\approx$water)	1500	1.5	10^{-8}
Muscle ($\approx$water)	1560	1.56	10^{-8}
Tallow ($\approx$fat)	390	0.39	10^{-4}

In the case of the point source of sound, the sound intensity of the radially propagating sound waves will obey the inverse square law [16], which yields spreading losses. In addition, the propagation medium absorbs the sound intensity with increasing r in terms of absorption losses (Chapter 3).
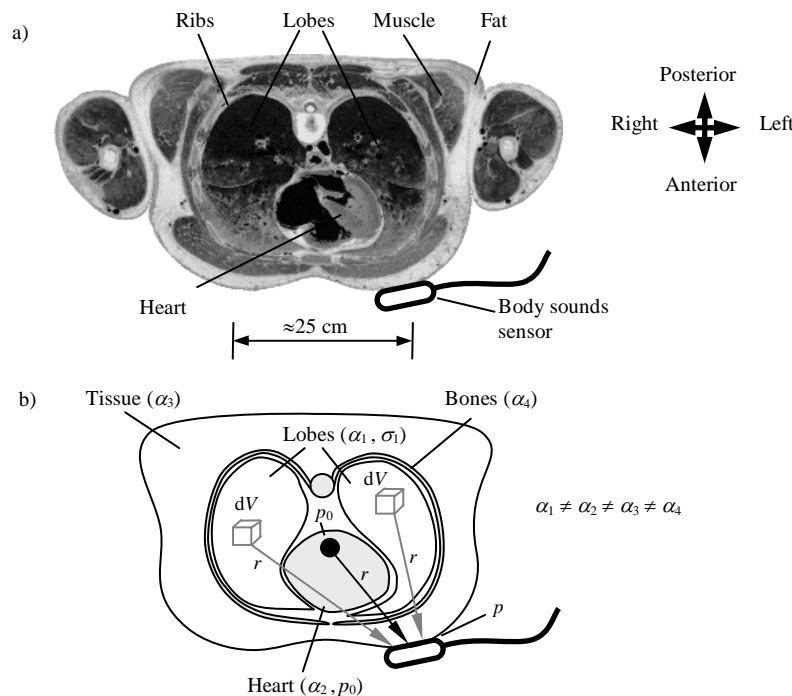

Fig. 1. **Propagation of the body sounds in a thorax. a) Cross-section of a thorax [21] in the height of the heart showing highly heterogeneous propagation medium. b) Contribution of the point source of sound (origin sound pressure p_0, Eq. 2) and the distributed sources of sound (volume elements dV with the respective volume density σ of the distributed sound pressure, Eq. 3) to the acoustic pressure p at the applied body sounds sensor as a function of the propagation distance r and the attenuation coefficients α**

Given both phenomena from above and assuming that the sound intensity is proportional to the square of the sound wave pressure p (strictly held only under far field conditions), the amplitude of p can be approximated as a function of r according to

$$p(r) = k \cdot \frac{p_0}{r} \cdot e^{-\alpha(r) \cdot r}. \qquad (2)$$

Here k is the constant, p_0 is the sound pressure amplitude of the point source at $r=0$, and $\alpha(r)$ is the sound absorption coefficient (Chapter 3.1) as a function of r. Here the geometrical damping factor $1/r$ comes from the inverse square law and looses its weight with increasing r while the original radial wave mutates into the plain wave.

Whereas Eq. 2 accounts for $p(r)$ from the point source of sound, the aforementioned distributed sources of sound can be considered by a modified version of Eq. 2, to give

$$p(r) = k \cdot \int_V \frac{\sigma(r)}{r} \cdot e^{-\alpha(r) \cdot r} dV, \qquad (3)$$

where $\sigma(r)$ represents the volume V density of the distributed sound pressure sources. Fig.1 demonstrates schematically the integration procedure for the highly heterogeneous thorax region (Fig.1a), showing inhomogeneously distributed $\alpha(r)$ (Fig.1b). The point source of sound with p_0 in the heart region as well as the distributed sources with local sound pressure $\sigma(r) \cdot dV$ in the lung parenchyma contribute to p at the auscultation site, i.e., the application region of the body sounds sensor.

2.2. Frequency dependant propagation

The peculiarities of the propagation pathway of the body sounds should be shortly addressed. In particular, the propagation pathway of the lung sounds differs with varying frequency. At relatively low frequencies, i.e., below 300 Hz [6] or in the frequency range (100-600) Hz [18], the transmission system of the lung sounds possesses primarily two features:

1) The large airway walls vibrate in response to intraluminal sound, allowing sound energy to be coupled directly into the surrounding parenchyma and inner mediastinum via wall motion.

2) The entire air branching networks behave approximately as non-rigid tubes which tend to absorb sound energy and thus to impede the sound traveling further into the branching structure.

As a result of the transmission peculiarities from above, the propagation pathway at the lower frequencies is primarily bound to the inner mediastinum, the sounds exiting the airways via wall motion. The lung parenchyma acts nearly as an elastic continuum to audible sounds which travel predominantly through the bulk of the parenchyma but not along the airways [19].

Contrary to the lower frequencies, the airway walls become rigid at the higher frequencies because of their inherent mass, allowing more sound energy to remain within the airway lumen and travel potentially further into the branching structure. Thus, the sounds at the higher frequencies tend to take the airway bound route within the airway-branching structure.

Given the varying pathway of the sound propagation for the different frequencies and the dependence of v on the propagation medium (Table 1), it can be deduced that v of the lung sounds at the lower frequencies is lower than v at the higher frequencies. This is because the sounds of the lower frequencies are bound to the parenchymal tissue with $v=50$ m/s and the sounds of the higher frequencies propagate primarily through the airways with $v=270$ m/s.

3. Attenuation of body sounds

Besides attenuation of the body sounds due to the spreading losses (see geometrical damping factor $1/r$ in Eq.2), the ability of sounds to travel through matter depends upon the intrinsic attenuation within the propagation medium. Generally, the attenuation phenomena include the following effects which will be discussed within the scope of the present chapter:

1. Volume effects, e.g., absorption;
2. In homogeneity effects, e.g., reflection and refraction.

3.1. Volume effects

Obviously the most important volume effect is the absorption which account for the loss or transformation of sound energy while passing through a material. The absorption process is represented quantitatively by α in Eq.2 (compare Fig.1) and accounts for the influence of all three [17, 18, 20, 22]:

1. Inner friction,
2. Thermal conduction,
3. Molecular relaxation.

The inner friction arises because of the differences in the local sound particle velocities. The friction strength is proportional to the ratio of the dynamic viscosity η to ρ, which shows that the transmission pathways with inertial components yield larger damping. The corresponding friction-related component α_F of α can be calculated as

$$\alpha_F = \frac{8 \cdot \pi^2 \cdot \eta}{3 \cdot \rho \cdot v^3} \cdot f^2 \qquad (4)$$

The value of α_F in the water is extremely low, e.g., $\alpha_F \approx 10^{-8}$ m^{-1} at 1 kHz. The latter value is also approximately applicable to the tissue which consists mainly of water (Table 1). In the air and large airways α_F increases by a factor of 1000 up to 10^{-5} m^{-1}.

The thermal conduction can be interpreted as diffusion of a kinetic energy. Since the propagation of the sound wave is linked with the local variations of temperature, the local balancing of these variations by the thermal conduction withdraws the energy from the wave. The coefficient α_T accounting for the above energy losses can be calculated as

$$\alpha_T = \left(\frac{c_P}{c_V} - 1 \right) \cdot \frac{2 \cdot \pi^2 \cdot \upsilon}{c_P \cdot \rho \cdot v^3} \cdot f^2, \qquad (5)$$

where c_P and c_V are the specific heat capacities at the constant pressure and volume, respectively, and υ is the heat conductivity. The value of α_T in water is lower than α_F in water by a factor of 1000, whereas α_T in air is in the some order as α_F in air.

The molecular relaxation contributes also to the acoustic absorption in the tissue. This phenomenon is based on the fact that the rapidly submitted energy from the sound field is primarily stored as rotational energy of atoms of involved molecules and, on the other hand, as translational energy which is proportional to the gas pressure. In contrast to the above energies, the vibrations of the molecules themselves start with some delay at the expense of rotational and translational energies. Thus a thermal equilibrium arises with a time constant τ (relaxation time) between these three types of energies. However, the delayed setting of this equilibrium yields energy losses, accounted by the absorption coefficient α_M

$$\alpha_M = \left(1 - \frac{v_0^2}{v_\infty^2}\right) \cdot \frac{2 \cdot \pi^2 \cdot \tau}{v \cdot \left(1 + (f/f_M)^2\right)} \cdot f^2 . \quad (6)$$

Here f_M $(=1/(2 \cdot \pi \cdot \tau))$ is the molecular relaxation frequency determined by the molecular properties, v_0 and v_∞ $(>v_0)$ are the sound velocities before relaxation $(f<<f_M)$ and after relaxation $(f>>f_M)$, respectively. In particular, the energy losses show a maximum at $f=f_M$ concerning the product $\alpha_M \cdot \lambda$. In the water, f_M shows a very high value of about 100 GHz. This high value of f_M $(>>2$ kHz$)$ induces a very small α_M of about 10^{-8} m^{-1} and a strong frequency dependence of α_M $(\propto f^2)$ in the frequency range of the body sounds (Chapter 1). The resulting value of α_M in the water is in the range of α_F in the water. Contrary to the water, the value of f_M in air is in the human acoustic range, the relaxation induced mainly by oxygen molecules ($f_M \approx 10$ Hz) and water molecules which content is given by the air humidity. Thus α_M in air is relatively large and amounts to about 10^{-3} m^{-1} at 1 kHz.

The total absorption α, as used in Eq.2, can be given as the sum of the discussed absorption coefficients, to give

$$\alpha = \alpha_F + \alpha_T + \alpha_M . \quad (7)$$

Table 1 compares α_F and α_T for the relevant types of biologic media involved in the sound transmission. It can be observed that the adipose tissue is the strongest absorber, followed by the air and airways, if only the inner friction and thermal conduction are considered. However, it should be stressed that α_F and α_T represent only the lowest threshold of the real absorption coefficient, the component α_M in Eq. 7 being usually larger than the sum $\alpha_F + \alpha_T$ by a few orders of magnitude.

If we consider the volume effects from a more practical point of view, the following observations can be made. An early paper [1] suggests that if the effects of the inner friction ($\approx \eta$, Eq. 4) are small, as in the case with water, air and bone, the sound energy may be transmitted with remarkably little losses. In other media, such as fatty breast tissue, the sound waves are almost immediately suppressed (compare Table 1). The flesh of the chest acts also as a significant damping medium since the obesity might completely mask the low frequency heart sounds [1], as will be demonstrated by own experimental data at the end of this chapter.

It is important to observe from Eqs. 4 and 5 that the sound absorption increases with increasing f, in particular, α_F and α_T are proportional to f^2. The obvious consequence is that the transmission efficiency of the lung parenchyma and the chest wall deteriorates with increasing f, i.e., the tissues act as a lowpass filter which transmits sounds mainly at low f [8, 18, 23, 24]. However, experimental data for the biological tissue suggest slightly different frequency dependence. That is, there are publications [5, 22, 25] which report that α is approximately proportional to f, whereas individual tissues may vary somewhat in between, e.g., hemoglobin has α proportional to $f^{1.3}$.

The non-continuous porous structure of the lung parenchyma is of a special importance regarding the frequency dependence of the sound absorption [16]. That is, the alveoli in the parenchyma act as elastic bubbles in the water, which dynamic deformation due to oscillating p dissipates the sound energy [20]. As long as λ (Table 1) is significantly greater than the alveolar size (diameter < 1mm), the losses are relatively low. In this case, the losses due to the thermal conduction are considerably larger in magnitude than those associated with the inner friction and scattering effects [18]. If the value of λ approaches alveolar size, i.e., f is increasing, the absorption exhibits very high losses [6]. However, it is important to note that the spectral range up to 2 kHz, i.e., the relevant spectral range of the body sounds (Chapter 1), yields values of λ which are still larger then the alveolar diameter. For instance, the alveolar size of λ in the lung parenchyma is approached earliest at f=23 kHz with v=23 m/s.

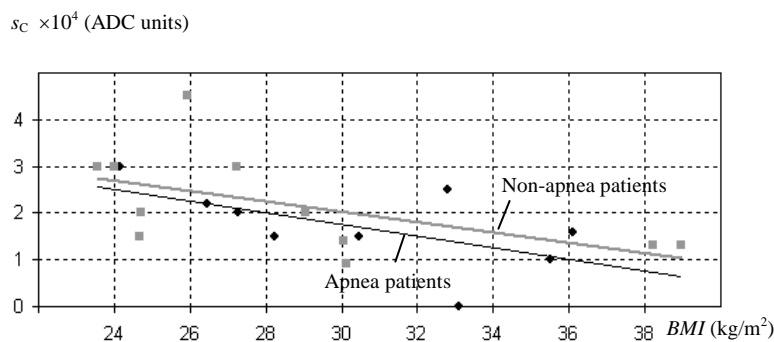$s_C \times 10^4$ (ADC units)

Fig. 2. **Relationship between the peak amplitude** s_C **of the heart sounds and the body mass index** *BMI* **for apnea patients (black) and non-apnea patients (grey), including corresponding linear regression lines**

Indeed, own experimental data gained with the body sounds sensor support the findings from above that the attenuation of the body sounds is significantly influenced by the volume effects. Fig.2 shows a regression analysis for the heart sounds, i.e., the regression between the peak amplitude s_C of the heart sounds and the body mass index *BMI* (anthropometric measure defined as weight in kilograms divided by the square of height in meters). Data of 20 patients were analysed; in total 9 patients had apnea (cessation of effective respiration during sleep). It can be deduced from the regression that increasing *BMI* is linked with decreasing s_C, an increase from 24 to 38 kg/m^2 causing about 60% loss of the amplitude, the cross-correlation coefficient being about -0.6. This might indicate that the increasing thickness of tissue and increasing amount of adipose tissue (in patients with higher *BMI*) yield a strong damping of the heart sounds.

Furthermore, the regression lines in Fig.2 indicate that s_C is slightly higher for the non-apnea patients in comparison with the apnea patients. This is in full agreement with the clinical signs of apnea [2, 3], including that the risk of apnea is strongly interrelated with the increased *BMI* and thus the decreased s_C.

3.2. Inhomogeneity effects

The inhomogeneity effects, namely, the reflection and refraction, play also an important role within the scope of the body sound attenuation. The spatial heterogeneity of the thorax that reflects the underlying anatomy, as demonstrated in Fig.1a, indicates the relevance of the intrathoracic sonic reflections and refractions. In addition, the tubelike resonances of the respiratory tract influence the attenuation of the body sounds [6].

The reflection phenomenon describes the relationship between the reflected and incident wave. If the reflection of the inner body sounds is considered on the skin (simplified tissue-air interface), as shown in Fig.3, then the reflection law yields the reflection coefficient R, i.e., the ratio of the reflected and incident p in the tissue, to give

$$R = \frac{Z_A - Z_T}{Z_A + Z_T} \qquad (8)$$

Here Z_A and Z_T are the sound radiation impedances ($=\rho \cdot v$) of the air and tissue, respectively. The calculation yields $Z_A \approx 340$ kg·m^{-2}·s^{-1} and $Z_T \approx 1.4 \cdot 10^6$ kg·m^{-2}·s^{-1}, whereas the physical properties of the tissue were approximated by those of the water. Given the values from above, Eq.8 yields $R \approx -0.998$. This very high value of R indicates that more than 99% of the incident p is reflected and less than 1% is transmitted through the skin if the simplified tissue-air interface is assumed.

A few restrictions should be mentioned regarding the above estimation of the reflection and transmission. The first restriction is that the human skin is a true multilayer consisting approximately of three layers: the inmost subcutaneous fat tissue, followed by the dermis, and the outer epidermis. Actually, the transmission of the body sounds through this multilayer would tend to yield a higher transmission rate compared with the simplified tissue-air interface. It is because of the assumption that the respective two neighboring layers would show a less difference in their sound radiation impedances Z_2 and Z_1 than the difference between Z_A and Z_T. As a result, the term $|Z_2 - Z_1|$ from Eq.8 would exhibit a lower value than the term $|Z_A - Z_T|$, which would yield a lower R for the respective neighboring layers and thus a higher total transmission rate.

The second restriction is that the reflection law holds only when λ of the sound is small compared to the dimensions of the reflecting surface, otherwise the scattering laws govern the reflection phenomena. Indeed, in the case of the body sounds, the application of the reflection law is limited, since λ (Table 1) and the dimensions of the reflecting surface (Fig.1) are in the same order. In spite of the above restrictions, the estimated low transmission efficiency (<1%) underlines the importance of an optimal sound auscultation region.
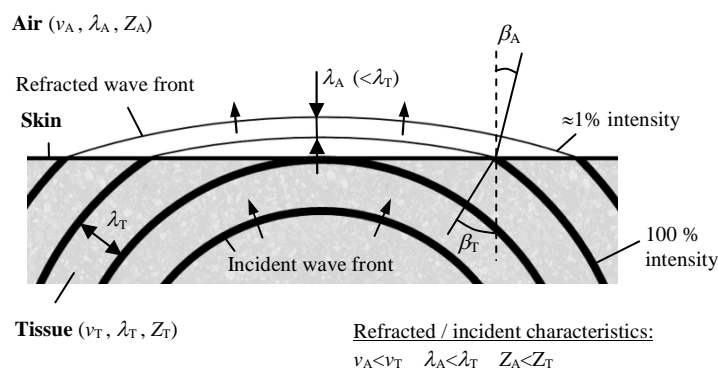

Air (v_A, λ_A, Z_A)

Refracted wave front

Skin

λ_A ($<\lambda_T$)

β_A

$\approx$1% intensity

λ_T

β_T

Incident wave front

100 % intensity

Tissue (v_T, λ_T, Z_T)

Refracted / incident characteristics:
$v_A < v_T \quad \lambda_A < \lambda_T \quad Z_A < Z_T$

Fig. 3. **Reflection losses and refraction of the body sounds when leaving the tissue. The decreasing thickness of the propagating wave front indicates the decreasing intensity due to the reflection losses**

The second inhomogeneity effect is the refraction which describes the bending of acoustic waves when they enter a medium where their v is different. Given the aforementioned simplified tissue-air interface, as demonstrated in Fig.3, the refraction angle β_A and the incident angle β_T obey the refraction law which yields $\beta_A < \beta_T$, given the values from Table 1. This means that the refracted wave front of the body sounds is bent towards the normal of the skin, which yields a more flat wave front in the air than in the tissue (Fig.3). From a practical point of view, the flattened wave front in the air favours the sounds auscultation, for the wave front is bunched and redirected towards the body sounds sensor on the skin. Lastly, it should be mentioned that the discussed restrictions pertaining to the reflection also apply to the refraction phenomenon.

3.3. Concluding remarks

The described biomechanical mechanisms of the sound propagation reveal that a large percentage of the original sound energy never reaches the surface because of spreading, absorption, scattering, reflection, and refraction losses. In particular, the sound attenuation within the body is highly inhomogeneous due to the heterogeneous thorax composition, and it increases generally with an increasing sound frequency. As a result, the high frequency sounds are more regionally restricted and play an important role in localizing, for instance, the breath sounds to underlying pathology.

Interestingly, the spatial propagation pathway of the sound waves depends on their frequency. That is, the low frequency sounds are predominantly bound to the inner mediastinum while the high frequency sounds tend to take an airway bound route. The different pathways have a strong influence on the resulting sound propagation velocity and wavelength, determining the type of acoustic field (near or far) on the auscultation site and, on the other hand, the strength of the prevailing scattering, reflection, and refraction effects.

The discussed unique transmission of the body sounds offers a solid basis for proper understanding of the relevance of the auscultated sounds and the optimization of the acoustic recording techniques.

References

1. **Rappaport M. B. and Sprague H. B.** Physiologic and physical laws that govern auscultation, and their clinical application. The acoustic stethoscope and the electrical amplifying stethoscope and stethograph. Am. Heart. J. 1941. Vol. 21(3). P. 257-318.
2. **Kaniusas E., Pfützner H. and Saletu B.** Acoustical signal properties for cardiac/respiratory activity and apneas. IEEE Trans. Biomed. Eng. 2005. Vol. 52(11). P. 1812-1822.
3. **Saletu B. and Saletu-Zyhlarz M.** What you always wanted to know about the sleep (in German). Ueberreuter Publisher, Vienna. 2001.
4. University of Wales, College of Medicine, Cardiac Auscultation Site (http://mentor.uwcm.ac.uk:11280/aspire/cardiac_auscultation/notes/part_2/the_audio_section/, 2005).
5. **Loudon R. and Murphy R. L. H.** Lung sounds. Am. Rev. Respir. Dis. 1984. Vol. 130(4). P. 663-673.
6. **Pasterkamp H., Kraman S. S. and Wodicka G. R.** Respiratory sounds, advances beyond the stethoscope. Am. J. Respir. Crit. Care Med. 1997. Vol. 156(3). P. 974-987.
7. **Dalmay F., Antonini M. T., Marquet P. and Menier R.** Acoustic properties of the normal chest. Eur. Respir. J. 1995. Vol. 8(10). P. 1761-1769.
8. **Kompis M., Pasterkamp H. and Wodicka G. R.** Acoustic imaging of the human chest. Chest 2001. Vol. 120. P. 1309-1321.
9. **Fachinger P.** Computer based analysis of lung sounds in patients with pneumonia - Automatic detection of bronchial breathing by Fast-Fourier-Transformation (in German). Dissertation at Philipps-University Marburg, 2003.
10. **Liistro G., Stanescu D. and Veriter C.** Pattern of simulated snoring is different through mouth and nose. J. Appl. Physiol. 1991. Vol. 70(6). P. 2736-2741.
11. **Beck R., Odeh M., Oliven A. and Gavriely N.** The acoustic properties of snores. Eur. Respir. J. 1995. Vol. 8(12), P. 2120-2128.
12. **Perez-Padilla J. R., Slawinski E., Difrancesco L. M., Feige R. R., Remmers J. E. and Whitelaw W. A.** Characteristics of the snoring noise in patients with and without occlusive sleep apnea. Am. Rev. Respir. Dis. 1993. Vol. 147(3). P. 635-644.
13. **Series F., Marc I. and Atton L.** Comparison of snoring measured at home and during polysomnographic studies. Chest 1993. Vol. 103(6). P. 1769-1773.
14. **Kompis M., Pasterkamp H., Oh Y., Motai Y. and Wodicka G. R.** Spatial representation of thoracic sounds. Proc. of the 20th annual EMBS International Conference, 1998. Vol. 20(3). P. 1661-1664.
15. **Pasterkamp H., Patel S. and Wodicka G. R.** Asymmetry of respiratory sounds and thoracic transmission. Med. Biol. Eng. Comput. 1997. Vol. 35(2). P. 103-106.
16. **Veit I.** Technical acoustics (in German). Vogel Publisher, Würzburg. 1996.
17. **Trendelenburg F.** Introduction into acoustic (in German). Springer Publisher, Berlin. 1961.
18. **Wodicka G. R., Stevens K. N., Golub H. L., Cravalho E. G. and Shannon D. C.** A model of acoustic transmission in the respiratory system. IEEE Trans. Biomed. Eng. 1989. Vol. 36(9). P. 925-934.
19. **Rice D. A.** Sound speed in pulmonary parenchyma. J. Appl. Physiol. 1983. Vol. 54(1). P. 304-308.
20. **Meyer E. and Neumann E. G.** Physical and technical acoustic (in German). Vieweg Publisher, Braunschweig. 1975.
21. **Bulling A., Castrop F., Agneskirchner J. D., Ovtscharoff W. A., Wurzinger L. J. and Gratzl M.** Body explorer. Springer Publisher, CD-ROM. 1997.
22. **Erikson K. R., Fry F. J. and Jones J. P.** Ultrasound in medicine - A review. IEEE Trans. Son. Ultrason. 1974. Vol. 21(3). P. 144-170.
23. **Welsby P. D. and Earis J. E.** Some high pitched thoughts on chest examination. Postgrad. Med. J. 2001. Vol. 77. P. 617-620.
24. **Welsby P. D., Parry G. and Smith D.** The stethoscope: Some preliminary investigations. Postgrad. Med. J. 2003. Vol. 79. P. 695-698.
25. **Hadjileontiadis L. J. and Panas S. M.** Adaptive reduction of heart sounds from lung sounds using fourth-order statistics. IEEE Trans. Biomed. Eng. 1997. Vol. 44(7). P. 642-648.

E. Kaniušas

Žmogaus kūno garsų perdavimas: apžvalga

Reziumė

Registruojamieji akustiniai kūno garsai yra svarbūs nustatant diagnozę. Kūno garsų sklidimas nuo židinio iki jų registracijos vietos nulemia registruoto akustinio biosignalo charakteristikas. Ši publikacija apžvelgia unikalų kūno garsų sklidimą ir jų slopinimą, parodo, kaip heterogeninė kūno struktūra ir garsų dažnis veikia garsų sklidimo kelią ir garsų charakteristikas. Fenomenalus kūno garsų sklidimas leidžia įžvelgti kliniškai svarbų ryšį tarp dominančio fiziologinio reiškinio ir registruojamo signalo. Be to, šis sklidimas parodo biosignalų reikšmingumą ir suteikia galimybę tobulinti kūno garsų registravimo techniką.